Reciprocity Constraints on Reflection

Cheng Guo[1,*] and Shanhui Fan[2,†]
[1]Department of Applied Physics, Stanford University, Stanford, California 94305, USA
[2]Ginzton Laboratory and Department of Electrical Engineering, Stanford University, Stanford, California 94305, USA

(Received 27 March 2022; accepted 7 June 2022; published 21 June 2022)

Reciprocity is a fundamental symmetry of Maxwell's equations. It is known that reciprocity imposes constraints on transmission, absorption, and emission. Here, we reveal reciprocity constraints on reflection. We determine the sets of all attainable reflection coefficients of n-port scattering matrices with prescribed singular values, both with and without assuming reciprocity. Their difference establishes reciprocity constraints and nonreciprocal behaviors. As an application, we examine the conditions for all-zero reflections. Our results deepen the understanding of reciprocity in optics.

DOI: 10.1103/PhysRevLett.128.256101

Lorentz reciprocity is a fundamental internal symmetry of Maxwell's equations [1–6]. It imposes direct constraints on transmission, absorption, and emission: When a system satisfies Lorentz reciprocity, the transmission between any two ports must be symmetric [7], and the absorptivity in each port must equal the corresponding emissivity [8,9]. Reciprocity constraints are essential in understanding photonic transport [10–12]. In contrast, systems breaking Lorentz reciprocity enable unique nonreciprocal phenomena [13,14] such as isolation [15–21], circulation [22], robust topological transport [23–26], and violation of Kirchhoff's law [27,28]. Thus, it is crucial to understand the fundamental role of reciprocity in basic phenomena.

In this Letter, we study reciprocity constraints on reflection. We consider a general linear time-invariant electromagnetic system [Fig. 1(a)]. The system can be lossy, lossless, or with gain. It is connected to its exterior by n ports. Describing the incoming and outgoing waves as

$$\boldsymbol{a} = (a_1, \ldots, a_n)^T, \qquad \boldsymbol{b} = (b_1, \ldots, b_n)^T, \tag{1}$$

where a_i and b_i are the input and output wave amplitudes in the ith port, respectively. The system is then described by a scattering matrix S of size $n \times n$:

$$\boldsymbol{b} = S\boldsymbol{a}, \qquad S = \begin{pmatrix} r_1 & t_{12} & \cdots & t_{1n} \\ t_{21} & r_2 & \cdots & t_{2n} \\ \vdots & \vdots & \ddots & \vdots \\ t_{n1} & t_{n2} & \cdots & r_n \end{pmatrix}. \tag{2}$$

Here, r_i is the reflection coefficient in the ith port [29], and t_{ij} is the transmission coefficient from the jth to the ith port. In general, S can be an arbitrary complex matrix. When the system has symmetries, S must satisfy the corresponding constraints. In particular, if the system is lossless, S must be unitary [7]. If the system is reciprocal, S must be symmetric [6,7]:

$$S = S^T. \tag{3}$$

From Eqs. (2) and (3), the existence of any reciprocity constraint on reflection may appear as a surprise: The reflection coefficients appear on the diagonal of S and thus are not obviously affected by Eq. (3). As a known example that hints at the existence of such a constraint, we consider a simple three-port lossless system with C_3 symmetry [Fig. 1(b)]. Without assuming reciprocity, its S matrix takes the form

$$S = \begin{pmatrix} r & t_1 & t_2 \\ t_2 & r & t_1 \\ t_1 & t_2 & r \end{pmatrix}, \tag{4}$$

where r can take any complex number with $|r| \leq 1$. If the system is further assumed to be reciprocal, then $t_1 = t_2$. It has been shown [31,32] that, in this case,

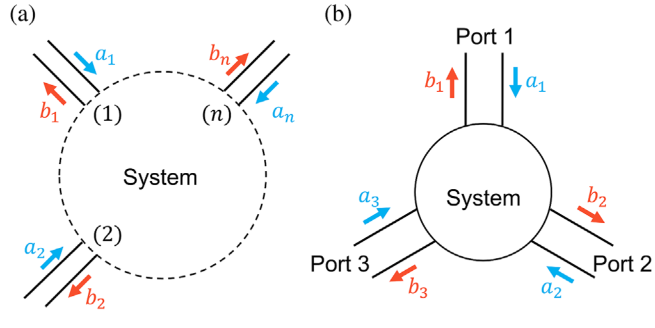

FIG. 1. (a) A general n-port system. (b) A 3-port lossless system with C_3 symmetry.

$$|r| \geq \frac{1}{3}. \tag{5}$$

Thus, $|r| < (1/3)$ can only occur in nonreciprocal systems. This example indicates that there exist reciprocity constraints on reflection.

Here, we study reciprocity constraints on reflection for general n-port systems. Using Thompson's theorems in matrix analysis [33,34], we completely determine the sets of all attainable reflection coefficients for n-port scattering matrices with prescribed singular values, in both the cases with and without assuming reciprocity. From this analysis, we establish the reciprocity constraints on reflection and provide the criteria for nonreciprocal phenomena. As one application, we examine the possibility for a device to exhibit zero reflection in every port. We show that if the device is lossless, it must be nonreciprocal for $n = 3$ but can be reciprocal for other values of $n > 1$. Our results reveal unrecognized consequences of reciprocity and deepen the understanding of optical transport through photonic structures.

Before presenting our results, we summarize useful notations. First, we provide some notations about the S matrix in Eq. (2). We refer to $r \equiv (r_1, r_2, \ldots, r_n)$ as the "reflection coefficient vector." Since the phases of r_i can be arbitrarily set by varying reference planes [7], we mainly focus on the magnitude $|r_i|$ and denote $|r| \equiv (|r_1|, |r_2|, \ldots, |r_n|)$. The system's dissipative property is characterized by the singular values of S: $\sigma(S) \equiv (\sigma_1, \sigma_2, \ldots, \sigma_n)$, listed in nonincreasing orders. (A singular value of a matrix S is the nonnegative square root of an eigenvalue of the matrix $S^\dagger S$ [35].) $(1 - \sigma_i^2)$ is directly related to the absorptivity [36]. We refer to $\sigma(S)$ as the "singular value vector." For lossless systems, all σ_i are 1. Then, we provide some mathematical notations. Let $x = (x_1, x_2, \ldots, x_n) \in \mathbb{R}^n$. We define $x^\downarrow = (x_1^\downarrow, x_2^\downarrow, \ldots, x_n^\downarrow)$, where $x_1^\downarrow \geq x_2^\downarrow \geq \cdots \geq x_n^\downarrow$ reorder the components of x in nonincreasing order. We also assume that empty sum is zero: $\sum_1^0 = 0$.

Now we discuss our main results. First, we consider lossless systems. We denote by $A[n]$ the set of attainable r for all n-port lossless systems without assuming reciprocity, and by $B[n]$ the corresponding set for *reciprocal* lossless systems. Obviously $B[n] \subseteq A[n]$. If $B[n] \neq A[n]$, there exist reciprocity constraints on reflection. Namely, there are reflection coefficients that are attainable only if reciprocity is broken.

To determine the reciprocity constraints, we apply Thompson's theorems [33,34] as summarized in the Supplemental Material (SM) [37], Sec. I, and obtain

$$A[n] = \left\{ r \in \mathbb{C}^n : |r|_1^\downarrow \leq 1, \sum_{i=1}^{n-1} |r|_i^\downarrow - |r|_n^\downarrow \leq n - 2 \right\}, \tag{6}$$

$$B[n] = \left\{ r \in A[n] : \sum_{i=1}^{n-3} |r|_i^\downarrow - \sum_{i=n-2}^{n} |r|_i^\downarrow \leq n - 4 \right\}, \tag{7}$$

where the condition in Eq. (7) is absent when $n = 1, 2$.

We illustrate the physical implications of these results. Equations (6) and (7) completely characterize the sets of attainable reflection coefficients for all general and reciprocal lossless systems, respectively.

When $n = 1, 2$, $B[n] = A[n]$: There is no reciprocity constraint. Specifically,

$$B[1] = A[1] = \{ r \in \mathbb{C} : |r| = 1 \}, \tag{8}$$

$$B[2] = A[2] = \{ r \in \mathbb{C}^2 : |r_1| = |r_2| \leq 1 \}. \tag{9}$$

Equations (8) and (9) are well-known for 1-port and 2-port lossless systems. When $n \geq 3$, $B[n] \subsetneqq A[n]$: There is a single reciprocity constraint as given in Eq. (7). Any violation of that inequality is a nonreciprocal effect.

For example, when $n = 3$,

$$A[3] = \{ r \in \mathbb{C}^n : |r|_1^\downarrow \leq 1, |r|_1^\downarrow + |r|_2^\downarrow - |r|_3^\downarrow \leq 1 \}, \tag{10}$$

$$B[3] = \{ r \in A[3] : |r_1| + |r_2| + |r_3| \geq 1 \}. \tag{11}$$

Figures 2(a) and 2(b) show the sets of attainable $(|r_1|, |r_2|, |r_3|)$ for 3-port general and reciprocal lossless systems, respectively. Both sets are convex polyhedra embedded inside a unit cube, with C_{3v} symmetry around the [111] direction. The former is a triangular bipyramid. The latter is a regular tetrahedron. Their difference is a tetrahedron with a volume of $(1/6)$.

The above geometric interpretation can be generalized to $n > 3$. Equations (6) and (7) indicate that the set of attainable $|r|$ is an intersection of finitely many closed half-spaces in $\mathbb{R}^n$ in both general and reciprocal cases. Each set is a bounded convex n-polytope [38] that is invariant under any permutation of coordinates. The reciprocity constraint in Eq. (7) corresponds to $\binom{n}{3}$ half-spaces, which

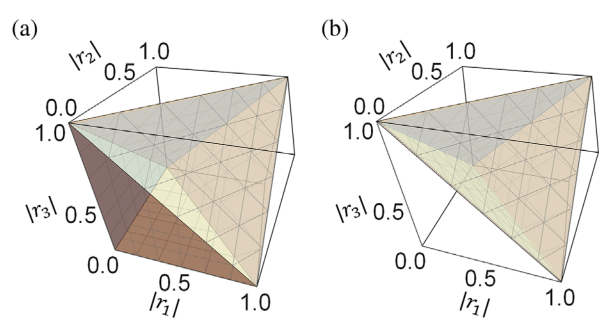

FIG. 2. Attainable $(|r_1|, |r_2|, |r_3|)$ for 3-port (a) lossless systems, (b) reciprocal lossless systems.

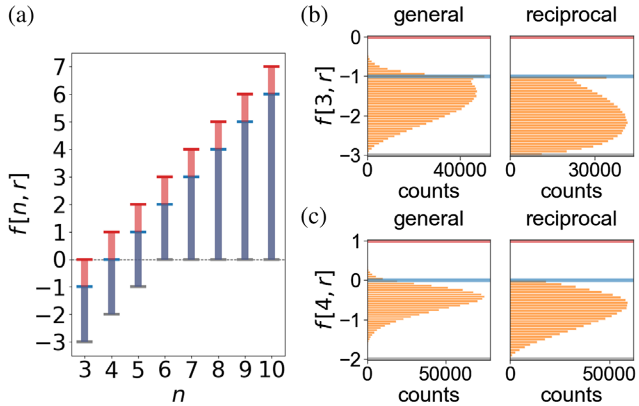

FIG. 3. (a) The range of $f[n,r]$. Blue intervals: $I_B[n]$. Union of blue and red intervals: $I_A[n]$. Red intervals: nonreciprocal effects. (b),(c) Histograms of $f[n,r]$ for 1 000 000 random n-port lossless systems: (b) $n=3$, (b) $n=4$. Red, blue, and gray lines indicate general upper bounds, reciprocal upper bounds, and lower bounds, respectively.

further bound the polytope for general systems and produce a smaller polytope for reciprocal systems.

Equation (7) suggests introducing a criterion function:

$$f[n,r]=\sum_{i=1}^{n-3}|r|_i^{\downarrow}-\sum_{i=n-2}^{n}|r|_i^{\downarrow}. \tag{12}$$

We prove that when $n\geq 3$, the range of $f[n,r]$ for all $r\in A[n]$ is

$$I_A[n]=[\min\{n-6,0\},n-3]; \tag{13}$$

the range of $f[n,r]$ for all $r\in B[n]$ is

$$I_B[n]=[\min\{n-6,0\},n-4]. \tag{14}$$

$I_B[n]\subsetneqq I_A[n]$ confirms $B[n]\subsetneqq A[n]$ when $n\geq 3$. The proofs of Eqs. (13) and (14) can be found in SM, Sec. II. We plot $I_A[n]$ and $I_B[n]$ in Fig. 3, where the red intervals correspond to nonreciprocal effects.

We further illustrate the probability distribution for the values of $f[n,r]$. Figures 3(b),(c) show the histograms of $f[3,r]$ and $f[4,r]$ for 1 000 000 random unitary matrices U_i and $\tilde{U}_i=U_iU_i^T$. Note $\tilde{U}_i$ is symmetric. Here, U_i is drawn from circular unitary ensemble with Haar measure [39], which provides a uniform probability distribution on $U(n)$. The horizontal lines indicate the theoretical bounds. In each case, the values of $f[n,r]$ tend to fill the entire predicted intervals. We also observe anomalous peaks in Fig. 3(b) but not in Fig. 3(c). The reason for this needs further investigation.

Now we explicitly construct a set of S matrices for which the values of $f[n,r]$ cover the whole intervals of $I_A[n]$ and $I_B[n]$, respectively. Such constructions are not unique; other matrices may also reach the bounds. For general lossless systems, consider three families of $n\times n$ matrices for $n\geq 3$:

$$I_n,\quad C_n=\begin{pmatrix}0&1&0&\cdots&0\\0&0&1&\cdots&0\\\vdots&\vdots&\vdots&\ddots&\vdots\\0&0&0&\cdots&1\\1&0&0&\cdots&0\end{pmatrix},\quad D_n=\begin{pmatrix}I_{n-3}&0\\0&C_3\end{pmatrix}, \tag{15}$$

where I_n is the n-identity matrix. All these matrices are unitary and thus characterize some lossless systems: I_n characterizes an n-port perfect reflector, C_n an n-port circulator, D_n an $(n-3)$-port perfect reflector combined with a 3-port circulator. Moreover, $f[n,r]=n-6$, 0, and $n-3$ for I_n, C_n, and D_n, respectively. We choose $U_{n,u}$ as D_n for any $n\geq 3$ to reach the upper bound of $I_A[n]$. We choose $U_{n,l}$ as I_n when $3\leq n<6$ or C_n when $n\geq 6$ to reach the lower bound of $I_A[n]$. For each $n\geq 3$, we define a skew-Hermitian matrix,

$$J_n=\log\left(U_{n,u}U_{n,l}^{\dagger}\right), \tag{16}$$

then construct a continuous path in $U(n)$ between $U_{n,l}$ and $U_{n,u}$:

$$U_n(\tau)\equiv e^{J_n\tau}U_{n,l},\qquad 0\leq\tau\leq 1. \tag{17}$$

By continuity, the values of $f[n,r]$ for $U_n(\tau)$ will cover the whole interval of $I_A[n]$.

For reciprocal lossless systems, we denote

$$M_5=\begin{pmatrix}0&\frac{1}{2}&z&-z&-\frac{1}{2}\\\frac{1}{2}&0&\frac{1}{2}&z&-z\\z&\frac{1}{2}&0&\frac{1}{2}&z\\-z&z&\frac{1}{2}&0&\frac{1}{2}\\-\frac{1}{2}&-z&z&\frac{1}{2}&0\end{pmatrix},\quad z=\frac{1-\sqrt{3}i}{4}. \tag{18}$$

M_5 corresponds to perhaps the simplest 5-port device that is lossless, reciprocal, and with all-zero reflection. M_5 is a Toeplitz matrix [35] with many symmetries. Then we introduce three additional families of $n\times n$ matrices:

$$E_n=\begin{pmatrix}I_{n-2}&0\\0&C_2\end{pmatrix};\quad F_n=\begin{pmatrix}C_2&&0\\&\ddots&\\0&&C_2\end{pmatrix},\quad n\text{ even}; \tag{19}$$

$$G_n = \begin{pmatrix} C_2 & & & 0 \\ & \ddots & & \\ & & C_2 & \\ 0 & & & M_5 \end{pmatrix}, \qquad n = 7, 9, \ldots. \tag{20}$$

All these matrices are symmetric and unitary and thus characterize some reciprocal lossless systems. Moreover, $f[n, r] = n - 6, n - 3,$ 0 and 0 for I_n, E_n, F_n, and G_n, respectively. We choose $\tilde{U}_{n,u}$ as E_n for any $n \geq 3$ to reach the upper bound of $I_n[B]$. We choose $\tilde{U}_{n,l}$ as I_n when $3 \leq n < 6$, or F_n when $n \geq 6$ and even, or G_n when $n \geq 6$ and odd, to reach the lower bound of $I_n[B]$. For each $n \geq 3$, we apply Takagi's decomposition [35,40] (see SM, Sec. III, for more details):

$$\tilde{U}_{n,l} = V_{n,l} V_{n,l}^T, \qquad \tilde{U}_{n,u} = V_{n,u} V_{n,u}^T. \tag{21}$$

Then we define a skew-Hermitian matrix,

$$K_n = \log\,(V_{n,u} V_{n,l}^\dagger), \tag{22}$$

and construct a continuous path between $\tilde{U}_{n,l}$ and $\tilde{U}_{n,u}$ in the space of $n \times n$ symmetric unitary matrices:

$$\tilde{U}_n(\tau) \equiv e^{K_n \tau} \tilde{U}_{n,l} e^{K_n^T \tau}, \qquad 0 \leq \tau \leq 1. \tag{23}$$

By continuity, the values of $f[n, r]$ for $\tilde{U}_n(\tau)$ will cover the whole interval of $I_B[n]$.

We proceed to study generic systems with loss or gain. The modification of reflection due to loss or gain has been extensively discussed in the literature [41–44]. We compare systems with the same singular values and hence the same dissipative property [36]. We denote by $A[n, \sigma]$ the set of attainable r for all n-port systems with a prescribed $\sigma \in \mathbb{R}^n$, and by $B[n, \sigma]$ the corresponding set for *reciprocal* systems. We apply Thompson's theorems [33,34] and obtain

$$A[n,\sigma] = \Bigg\{ r \in \mathbb{C}^n : \sum_{i=1}^{k} |r|_i^{\downarrow} \leq \sum_{i=1}^{k} \sigma_i, 1 \leq k \leq n; \\ \sum_{i=1}^{n-1} |r|_i^{\downarrow} - |r|_n^{\downarrow} \leq \sum_{i=1}^{n-1} \sigma_i - \sigma_n \Bigg\}, \tag{24}$$

$$B[n,\sigma] = \Bigg\{ r \in A[n,\sigma] : \sum_{i=1}^{k-1} |r|_i^{\downarrow} - \sum_{i=k}^{n} |r|_i^{\downarrow} \leq \sum_{i \neq k} \sigma_i - \sigma_k, \\ 1 \leq k \leq n-1; \sum_{i=1}^{n-3} |r|_i^{\downarrow} - \sum_{i=n-2}^{n} |r|_i^{\downarrow} \leq \sum_{i=1}^{n-2} \sigma_i - \sum_{i=n-1}^{n} \sigma_i \Bigg\}. \tag{25}$$

The last condition in Eq. (25) is absent when $n = 1$, 2.

We illustrate the physical implications of these results. Equations (24) and (25) completely characterize all attainable reflection coefficients for general and reciprocal systems, respectively, with prescribed singular values σ.

When $n = 1$, there is no reciprocity constraint:

$$B[1, \sigma] = A[1, \sigma] = \{ r \in \mathbb{C} : |r| = \sigma_1 \}. \tag{26}$$

When $n = 2$, if $\sigma_1 = \sigma_2$, there is no reciprocity constraint:

$$B[2, \sigma] = A[2, \sigma] = \{ r \in \mathbb{C}^2 : |r_1| = |r_2| \leq \sigma_1 \}. \tag{27}$$

Equation (27) reduces to Eq. (9) when $\sigma_1 = \sigma_2 = 1$. If $\sigma_1 \neq \sigma_2$, there is a single reciprocity constraint:

$$|r_1| + |r_2| \geq \sigma_1 - \sigma_2. \tag{28}$$

As an illustration, Figs. 4(a) and 4(b) show the sets of attainable $(|r_1|, |r_2|)$ for 2-port general and reciprocal systems, respectively, with $\sigma = (0.70, 0.32)$. Both sets are convex polygons with mirror symmetry about the [11] axis. The former is a pentagon. The latter is a rectangle. Their difference is an isosceles right triangle.

When $n \geq 3$, there are in general n reciprocity constraints on reflection as given in Eq. (25). Depending on σ, some of the inequalities may be redundant. As an illustration, Figs. 5(a) and 5(b) show the sets of attainable $(|r_1|, |r_2|, |r_3|)$ for 3-port general and reciprocal systems, respectively, with $\sigma = (0.9, 0.7, 0.5)$. Both sets are convex polyhedra with C_{3v} symmetry around the [111] direction. The former is a decahedron. The latter is a tetradecahedron.

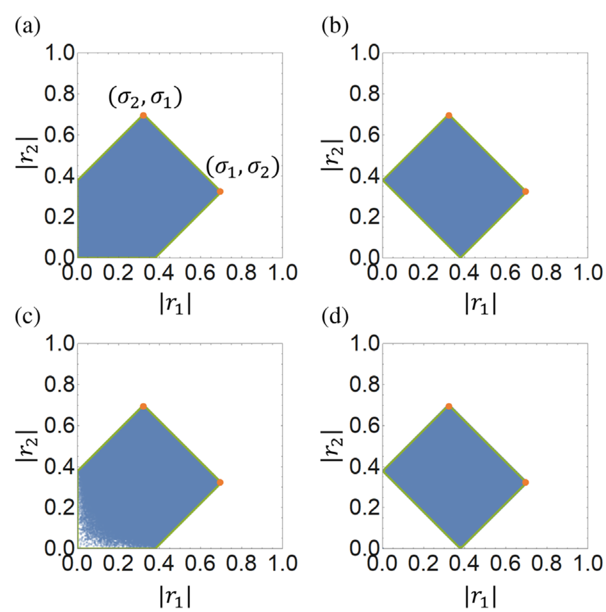

FIG. 4. Attainable $(|r_1|, |r_2|)$ for 2-port systems with $\sigma = (0.70, 0.32)$. (a) General systems. (b) Reciprocal systems. (c),(d) Numerical results of 200 000 random samples.

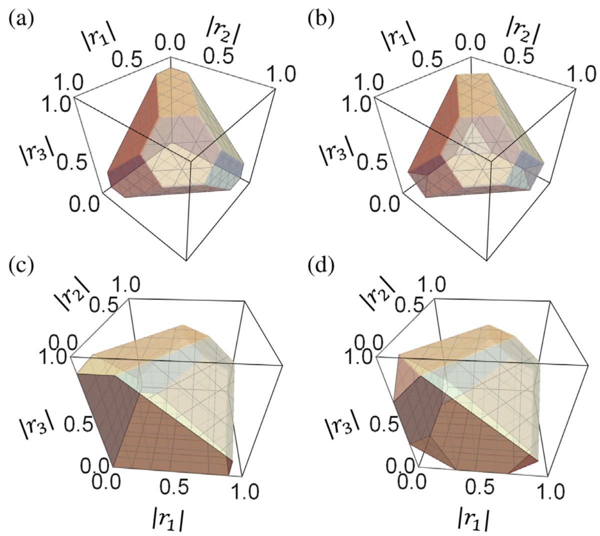

FIG. 5. Attainable $(|r_1|, |r_2|, |r_3|)$ for 3-port systems with $\sigma = (0.9, 0.7, 0.5)$. (a) General systems. (b) Reciprocal systems. (c),(d) A different view of (a),(b).

Their difference consists of four tetrahedra. This is more evident in Figs. 5(c) and 5(d).

Here, we emphasize that the conditions characterizing $A[n]$, $B[n]$, $A[n,\sigma]$, and $B[n,\sigma]$ are both necessary and sufficient: Any value of r in the set is achievable; any value of r not in the set is not. As one illustration, see SM, Sec. IV, for explicit examples of S matrices for which $|r|$ reaches the vertices of the polytopes in Figs. 2, 4, and 5. As another illustration, Figs. 4(c) and 4(d) show $(|r_1|, |r_2|)$ of 200 000 random asymmetric and symmetric matrices with $\sigma = (0.70, 0.32)$, respectively. In each case, all the points are contained in the predicted region; the whole predicted region will be covered when more examples are considered. (See SM, Sec. V, for the histograms of $|r_1| + |r_2|$.)

We obtain similar numerical results for other n and σ.

As an application, we examine the possibility of all-zero reflection:

$$r = (0, \ldots, 0). \tag{29}$$

Such a property is desired in various photonic applications. It is necessary for an ideal cloak [45,46], which demands the complete absence of scattering. It differs from coherent perfect absorption [47], which demands the complete absorption, hence the absence of reflection, only for a specific incident wave. In the lossless cases, we substitute Eq. (29) into Eqs. (6) and (7) and deduce that all-zero reflection is possible when $n \neq 1$ for nonreciprocal systems, and when $n \neq 1, 3$ for reciprocal systems. Thus, a 3-port lossless device exhibiting all-zero reflections must be nonreciprocal. An example is a 3-port circulator as designed in both microwave [31] and optical frequencies [22]. For systems with gain or loss, we substitute Eq. (29) into Eqs. (24) and (25). We deduce that for nonreciprocal systems, all-zero reflection is possible when $n = 1$, $\sigma = 0$, and when $n \geq 2$, for all σ's. For reciprocal systems, all-zero reflection is possible if σ satisfies the following conditions: When $n = 1$, $\sigma = 0$; when $n = 2$, $\sigma_1 = \sigma_2$; when $n \geq 3$,

$$\sum_{i=2}^{n} \sigma_i - \sigma_1 \geq 0, \qquad \sum_{i=1}^{n-2} \sigma_i - \sigma_{n-1} - \sigma_n \geq 0. \tag{30}$$

We verify these criteria using previous examples. Figure 2 confirms the cases of 3-port lossless systems. Figure 4 confirms the cases of 2-port systems with $\sigma_1 \neq \sigma_2$. Figure 5 confirms the cases of 3-port systems with $\sigma = (0.9, 0.7, 0.5)$, where σ violates the second inequality of (30). C_n, F_n, and G_n in Eqs. (15), (19), and (20) are examples of lossless systems exhibiting all-zero reflection.

In conclusion, we determine all attainable reflection coefficients for general and reciprocal n-port electromagnetic systems with prescribed singular values. We establish the reciprocity constraints on reflection. We deduce the criteria for all-zero reflection. Our work elucidates the fundamental role of reciprocity in reflection and provides theoretical guidelines for practical photonic design. The theory can be readily extended to other classical and quantum wave systems described by scattering matrix formalisms, including acoustic and electronic waves.

C. G. thanks Zhaoyou Wang for helpful discussions. This work is supported by a Simons Investigator in Physics grant from the Simons Foundation (Grant No. 827065).

*Corresponding author.
guocheng@stanford.edu
†Corresponding author.
shanhui@stanford.edu

[1] H. A. Lorentz, The theorem of Poynting concerning the energy in the electromagnetic field and two general propositions concerning the propagation of light, Amst. Akad. Wet. **4**, 176 (1896).
[2] R. J. Potton, Reciprocity in optics, Rep. Prog. Phys. **67**, 717 (2004).
[3] D. Jalas, A. Petrov, M. Eich, W. Freude, S. Fan, Z. Yu, R. Baets, M. Popović, A. Melloni, J. D. Joannopoulos, M. Vanwolleghem, C. R. Doerr, and H. Renner, What is—and what is not—an optical isolator, Nat. Photonics **7**, 579 (2013).
[4] C. Caloz, A. Alù, S. Tretyakov, D. Sounas, K. Achouri, and Z.-L. Deck-Léger, Electromagnetic nonreciprocity, Phys. Rev. Applied **10**, 047001 (2018).
[5] V. S. Asadchy, M. S. Mirmoosa, A. Díaz-Rubio, S. Fan, and S. A. Tretyakov, Tutorial on electromagnetic nonreciprocity and its origins, Proc. IEEE **108**, 1684 (2020).

[6] C. Guo, Z. Zhao, and S. Fan, Internal transformations and internal symmetries in linear photonic systems, Phys. Rev. A **105**, 023509 (2022).

[7] H. A. Haus, *Waves and Fields in Optoelectronics* (Prentice-Hall, Englewood Cliffs, NJ, 1984).

[8] G. Kirchhoff, Ueber das Verhältniss zwischen dem Emissionsvermögen und dem Absorptionsvermögen der Körper für Wärme und Licht, Ann. Phys. (Berlin) **185**, 275 (1860).

[9] J.-J. Greffet, P. Bouchon, G. Brucoli, and F. Marquier, Light Emission by Nonequilibrium Bodies: Local Kirchhoff Law, Phys. Rev. X **8**, 021008 (2018).

[10] U. Rau, Reciprocity relation between photovoltaic quantum efficiency and electroluminescent emission of solar cells, Phys. Rev. B **76**, 085303 (2007).

[11] J. Luo, H. Chu, R. Peng, M. Wang, J. Li, and Y. Lai, Ultra-broadband reflectionless Brewster absorber protected by reciprocity, Light **10**, 89 (2021).

[12] H. Chu, X. Xiong, Y.-J. Gao, J. Luo, H. Jing, C.-Y. Li, R. Peng, M. Wang, and Y. Lai, Diffuse reflection and reciprocity-protected transmission via a random-flip metasurface, Sci. Adv. **7**, eabj0935 (2021).

[13] D. L. Sounas and A. Alù, Non-reciprocal photonics based on time modulation, Nat. Photonics **11**, 774 (2017).

[14] I. A. D. Williamson, M. Minkov, A. Dutt, J. Wang, A. Y. Song, and S. Fan, Integrated nonreciprocal photonic devices with dynamic modulation, Proc. IEEE **108**, 1759 (2020).

[15] Z. Yu and S. Fan, Complete optical isolation created by indirect interband photonic transitions, Nat. Photonics **3**, 91 (2009).

[16] L. Bi, J. Hu, P. Jiang, D. H. Kim, G. F. Dionne, L. C. Kimerling, and C. A. Ross, On-chip optical isolation in monolithically integrated non-reciprocal optical resonators, Nat. Photonics **5**, 758 (2011).

[17] M. S. Kang, A. Butsch, and P. S. J. Russell, Reconfigurable light-driven opto-acoustic isolators in photonic crystal fibre, Nat. Photonics **5**, 549 (2011).

[18] H. Lira, Z. Yu, S. Fan, and M. Lipson, Electrically Driven Nonreciprocity Induced by Interband Photonic Transition on a Silicon Chip, Phys. Rev. Lett. **109**, 033901 (2012).

[19] Z. Shen, Y.-L. Zhang, Y. Chen, C.-L. Zou, Y.-F. Xiao, X.-B. Zou, F.-W. Sun, G.-C. Guo, and C.-H. Dong, Experimental realization of optomechanically induced non-reciprocity, Nat. Photonics **10**, 657 (2016).

[20] V. S. Asadchy, C. Guo, B. Zhao, and S. Fan, Sub-wavelength passive optical isolators using photonic structures based on Weyl semimetals, Adv. Opt. Mater. **8**, 2000100 (2020).

[21] H. Tian, J. Liu, A. Siddharth, R. N. Wang, T. Blésin, J. He, T. J. Kippenberg, and S. A. Bhave, Magnetic-free silicon nitride integrated optical isolator, Nat. Photonics **15**, 828 (2021).

[22] Z. Wang and S. Fan, Optical circulators in two-dimensional magneto-optical photonic crystals, Opt. Lett. **30**, 1989 (2005).

[23] Z. Wang, Y. Chong, J. D. Joannopoulos, and M. Soljačić, Observation of unidirectional backscattering-immune topological electromagnetic states, Nature (London) **461**, 772 (2009).

[24] K. Fang, Z. Yu, and S. Fan, Realizing effective magnetic field for photons by controlling the phase of dynamic modulation, Nat. Photonics **6**, 782 (2012).

[25] L. Lu, J. D. Joannopoulos, and M. Soljačić, Topological photonics, Nat. Photonics **8**, 821 (2014).

[26] T. Ozawa, H. M. Price, A. Amo, N. Goldman, M. Hafezi, L. Lu, M. C. Rechtsman, D. Schuster, J. Simon, O. Zilberberg, and I. Carusotto, Topological photonics, Rev. Mod. Phys. **91**, 015006 (2019).

[27] L. Zhu and S. Fan, Near-complete violation of detailed balance in thermal radiation, Phys. Rev. B **90**, 220301(R) (2014).

[28] C. Guo, B. Zhao, and S. Fan, Adjoint Kirchhoff's Law and General Symmetry Implications for All Thermal Emitters, Phys. Rev. X **12**, 021023 (2022).

[29] This definition is standard in the literature on S matrices [7]. It implies that the backward reflection is in the same spatial channel as the incidence. In some photonic applications, special care needs to be taken to formulate the S matrices this way [30]. For example, for oblique light incidence on a surface, the conventional definition of reflection direction is different from the incident direction.

[30] Y. Guo, M. Xiao, and S. Fan, Topologically Protected Complete Polarization Conversion, Phys. Rev. Lett. **119**, 167401 (2017).

[31] K. Kurokawa, *An Introduction to the Theory of Microwave Circuits* (Academic, New York, 1969).

[32] S. Fan, S. G. Johnson, J. D. Joannopoulos, C. Manolatou, and H. A. Haus, Waveguide branches in photonic crystals, J. Opt. Soc. Am. B **18**, 162 (2001).

[33] R. C. Thompson, Singular values, diagonal elements, and convexity, SIAM J. Appl. Math. **32**, 39 (1977).

[34] R. Thompson, Singular values and diagonal elements of complex symmetric matrices, Linear Algebra Appl. **26**, 65 (1979).

[35] R. A. Horn and C. R. Johnson, *Matrix Analysis*, 2nd ed. (Cambridge University Press, New York, NY, 2017).

[36] D. A. B. Miller, L. Zhu, and S. Fan, Universal modal radiation laws for all thermal emitters, Proc. Natl. Acad. Sci. U.S.A. **114**, 4336 (2017).

[37] See Supplemental Material at http://link.aps.org/supplemental/10.1103/PhysRevLett.128.256101 for Thompson's theorems, proofs of Eqs. (13,14), Takagi's decomposition, examples of S matrices at the vertices of the convex polytopes in Figs. 2, 4, 5, and the histograms for Figs. 4(c,d).

[38] B. Grünbaum, V. Kaibel, V. Klee, and G. M. Ziegler, *Convex Polytopes*, 2nd ed. (Springer, New York, 2003).

[39] F. Mezzadri, How to generate random matrices from the classical compact groups, Not. Am. Math. Soc. **54**, 592 (2007).

[40] K. D. Ikramov, Takagi's decomposition of a symmetric unitary matrix as a finite algorithm, Comput. Math. Math. Phys. **52**, 1 (2012).

[41] S. Fan, P. R. Villeneuve, J. D. Joannopoulos, and H. A. Haus, Loss-induced on/off switching in a channel add/drop filter, Phys. Rev. B **64**, 245302 (2001).

[42] A. Guo, G. J. Salamo, D. Duchesne, R. Morandotti, M. Volatier-Ravat, V. Aimez, G. A. Siviloglou, and D. N. Christodoulides, Observation of PT-Symmetry Breaking in Complex Optical Potentials, Phys. Rev. Lett. **103**, 093902 (2009).

[43] A. Aiello, M. Merano, and J. P. Woerdman, Duality between spatial and angular shift in optical reflection, Phys. Rev. A **80**, 061801(R) (2009).

[44] P. Tassin, L. Zhang, T. Koschny, E. N. Economou, and C. M. Soukoulis, Low-Loss Metamaterials Based on Classical Electromagnetically Induced Transparency, Phys. Rev. Lett. **102**, 053901 (2009).

[45] U. Leonhardt, Optical conformal mapping, Science **312**, 1777 (2006).

[46] J. B. Pendry, D. Schurig, and D. R. Smith, Controlling electromagnetic fields, Science **312**, 1780 (2006).

[47] Y. D. Chong, L. Ge, H. Cao, and A. D. Stone, Coherent Perfect Absorbers: Time-Reversed Lasers, Phys. Rev. Lett. **105**, 053901 (2010).